Journal of Physical Chemistry & Biophysics

Cataldo et al., J Phys Chem Biophys 2014, 4:1
DOI: 10.4172/2161-0398.1000133

Research Article Open Access

Quantum Mechanical Modeling of Fluoromethylated-pyrrol Derivatives a Study on their Reactivities, Structures and Vibrational Properties

Pablo G. Cataldo, María V. Castillo and Silvia A. Brandán*

Cátedra de Química General, Instituto de Química Inorgánica, Facultad de Bioquímica, Química y Farmacia, Universidad Nacional de Tucumán, Ayacucho 471, 4000, San Miguel de Tucumán, Tucumán, R. Argentina

Abstract

In this work, the structural and vibrational properties of 1-5-(difluoromethyl-1H-pyrrol-2-yl-) ethanone (DFPE) were studied by using the hybrid B3LYP/6-31G* method. The properties were analyzed and compared with those obtained for 1-(1H-pyrrol-2-yl) ethanone (PE) and 1-(5-(trifluoromethyl)-1H-pyrrol-2-yl) ethanone (TFPE). The theoretical ^{1}H-NMR, ^{13}C-NMR and ^{19}F-NMR chemical shifts for DFPE were predicted by using the B3LYP/6-311++G** approach with the GIAO and CGST methods showing the three spectra good concordances with the corresponding experimental ones. A complete assignment of the vibrational spectra was presented.

Keywords: 1-5-(difluoromethyl-1H-pyrrol-2-yl-)ethanone; Vibrational spectra; Molecular structure; Force field; DFT calculations

Introduction

The difluoromethyl group (CF_2H) is normally used in areas as pharmacology and medicine because it has hydrogen bond donor properties of great importance in the drug design [1]. The hydrogen bond in this system may be related to the enhanced biological activity of the CF_2H compound over its CF_3 counterpart, as reported by Ericsson and Mc Loughlin [2], allowing this way, their incorporating in a wide variety of organic molecules [1]. In recent times, Fujiwara et al. [1] have reported a new reagent for direct difluoromethylation of organic substrates via a radical process, the zinc difluoro methyl sulfonate salt (ZnDFMS), $Zn(SO_2\ CF_2H)_2$, which allows the selective difluoromethylation of heteroarenes and related structures. Recently, the structural and vibrational studies and molecular force field of ZnDFMS were reported by Romano et al. [3], who for the compound have evidenced by means of the infrared and Raman spectra the presence of two coordination modes, monodentate and bidentate. In the theoretical structural and vibrational studies of the potential anticancer agent, 5- difluoromethyl-1,3,4-thiadiazole-2-amino [4], the DFT calculations and the experimental infrared spectrum in the solid state shown the presence of two tautomers of the compound. On the other hand, the pyrrol heterocyclic and some of their derivatives, such as indole, are broadly used as selective drugs for treatment of many diseases [5,6] and also, to build up conducting interfaces because their chemical or electrochemical polymerization is generally easy, resulting polymers robust and regular films [7]. Consequently, the compounds containing F atoms in their structures are important for the design of drugs and of novel and functional conducting polymer films [8,9]. Müller et al [10] have reported that the F atom can improve binding efficacy and selectivity of pharmaceuticals products because the fluorination of molecules often imparts desirable properties, such as the metabolic and thermal stability [11,12]. In these contexts, the knowing of the structures of compounds containing both, difluoromethyl and pyrrol groups are useful and necessary to predict their properties and behaviours in the different media in which they are involved and, also to perform the complete assignments of the corresponding vibrational spectra. Hence, these derivatives in any system can be easily identified by means of vibrational spectroscopy. In this work, we have studied from theoretical point of view the structure, the vibrational spectra and the structural properties of 1-5-(difluoromethyl-1H-pyrrol-2-yl-)ethanone (DFPE), a new fluoro methylated-pyrrol derivative synthesized by Fujiwara et al. [1] by using ZnDFMS as reagent and a unreported synthetic procedure. So far, the experimental structure of this compound, reported as a white solid, was not determined and only the experimental ^{1}H-NMR, ^{13}C-NMR, ^{19}F-NMR spectra and some observed bands in the infrared spectrum in solid phase were published [1]. Here, the initial structures of the different conformers of DFPE were modelled and optimized by using hybrid B3LYP/6-31G* calculations [13,14]. The nature of the interactions present in the structures were studied employing natural bond orbital (NBO) calculations [15,16] and the atoms in molecules theory (AIM) [17,18] while the reactivities of the more stable conformers were predicted by means of the highest occupied molecular orbital (HOMO)-lowest unoccupied molecular orbital (LUMO) energy gaps [19]. Here, the hydrogen bond donor properties for the CF_2H group of DFPE were analyzed by means of the molecular electrostatic potentials [20-23] and later, they were compared with those obtained for the same group of ZnDFMS [3] and 5-difluoromethyl-1,3,4- thiadiazole-2-amino [4] and, for those obtained in this work for 1-(1H-pyrrol-2-yl) ethanone (PE) and 1-(5-(trifluoromethyl)-1H-pyrrol-2-yl) ethanone (TFPE) [24,25]. The harmonic frequencies for DFPE and TFPE were also calculated and, later, at the same level of theory the detailed assignments of all the infrared bands were performed taking into account the scaled quantum mechanics force field methodology (SQMFF) [26] and the corresponding internal natural coordinates. The Raman spectra for DFPE and TFPE were predicted by using the hybrid B3LYP/6-31G* method. The theoretical ^{1}H-NMR, ^{13}C-NMR, ^{19}F-NMR spectra were calculated by using the Gauge-Independent Atomic Orbital (GIAO)

***Corresponding author:** Silvia A. Brandán, Cátedra de Química General, Instituto de Química Inorgánica, Facultad de Bioquímica, Química y Farmacia, Universidad Nacional de Tucumán, Ayacucho 471, 4000, San Miguel de Tucumán, Tucumán, R. Argentina, Tel: +54-381-4247752; Fax: +54-381-4248169; E-mail:sbrandan@fbqf.unt.edu.ar

Received January 17, 2014; **Accepted** February 26, 2014; **Published** February 28, 2014

Citation: Cataldo PG, Castillo MV, Brandán SA (2014) Quantum Mechanical Modeling of Fluoromethylated-pyrrol Derivatives a Study on their Reactivities, Structures and Vibrational Properties. J Phys Chem Biophys 4: 133. doi:10.4172/2161-0398.1000133

[27] and Continuous Set of Gauge Transformations (CSGT) [28] methods employing the optimized structures at B3LYP/6-311++G** level because it size of basis set is recommended for the NMR chemical shift calculations [29,30]. The calculated values show good concordance with the corresponding experimental ones.

Computational Details

For DFPE, three stable structures with C_1 symmetries were found in the potential energy surface by using the hybrid B3LYP/6-31G* method which are observed in the Figure 1 together with the numbering of all the atoms. These structures were initially modelled with the *Gauss View* 5.0 program [31] and, then, they were optimized by using the Gaussian 09 program package [32]. The study of the inter- and intra-molecular hydrogen-bonding interactions in DFPE is very important and useful to understand the connection between the structures and activities due to the presence of potentials hydrogen bond donors (N-H and CF_2H) and acceptors (C=O) groups, for these reasons, the NBO calculations were performed by using the NBO 3.1 program [16], as implemented in the Gaussian 09 package while for the AIM analysis the AIM200 program was employed [18].

On the other hand, in this work two different types of charges, such as the natural charges (NPA) and those MK's charges derived from Merz-Kollman [33] were analyzed. Besides, the bond orders expressed as Wiberg indexes and the stabilization energies for all the studied species were also calculated together with the corresponding molecular electrostatic potentials [20-23]. All the computed properties for the three conformers of DFPE were compared with those obtained at the same level of theory for PE and TFPE. In this work, the more stable structures of PE and TFPE are presented in Figure S1 (Supporting material). The harmonic frequencies and the force fields expressed in Cartesian coordinates for DFPE and TFPE were calculated at B3LYP/6-31G* level and, later, the resulting force fields were transformed to "natural" internal coordinates employing the Molvib program [34]. Tables S1 and S2 (Supporting material) shows the natural internal coordinates defined for all the conformers of DFPE and for the more stable structure of TFPE, in accordance with those obtained for molecules similar [3,4,35-38]. The complete vibrational assignments for DFPE and TFPE were performed with the SQMFF methodology and considering the potential energy distribution components (PED) ≥ 10%. The theoretical ^{1}H-NMR, ^{13}C-NMR and ^{19}F-NMR chemical shifts for the three conformers of DFPE were computed with the GIAO [27] and CGST methods [28] by using the geometries optimized at the B3LYP/6-311++G** level of theory and, by using, for the ^{1}H and ^{13}C atoms, TMS as reference while, for the ^{19}F atoms, CCl_3F was used as reference. Then, the calculated values were compared with the corresponding experimental ones. Finally, the chemical potential (μ), electronegativity (χ), global hardness (η), global softness (S) and global electrophilicity index (ω) descriptors [19] were calculated for the three conformers of DFPE by using the frontiers orbital in order to predict their behaviours and reactivities with electrophiles and/or nucleophiles. Later, the results for DFPE were compared with those obtained for PE and TFPE.

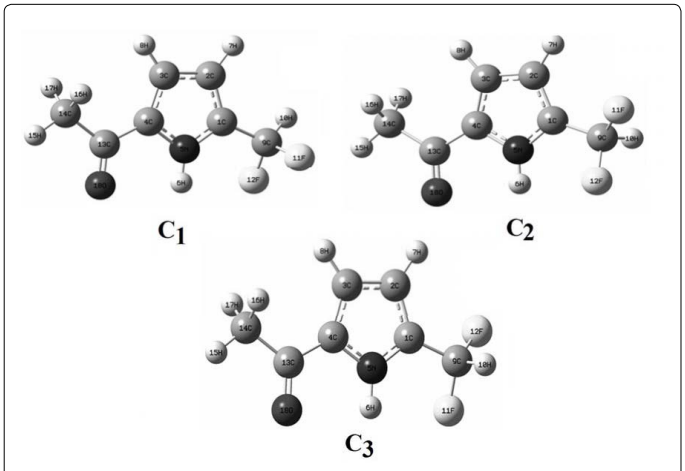

Figure 1: Molecular structures for the three stable conformers of 1-(5-(difluoromethyl) -1H-pyrrol-2-yl) ethanone (DFPE) with the labeling of atoms.

Results and Discussion

Geometry optimization

The total energies for the three stable structures of DFPE together with the corresponding dipole moment values by using the B3LYP/6-31G* method can be seen in Table S3 together with the corresponding values for PE and TFPE. Figures S2 and S3 show the positions of the dipole moments for the three stable structures of DFPE and for PE and TFPE, respectively. For DFPE, the results show that the C_I conformer is the most stable conformer in gas phase and, that, C_{II} and C_{III} have the same energy and dipole moment values, as can be seen in Figure S2. In fact, the low energy difference among them (0.18 kJ/mol) show that probably the three conformers are present in the gas phase at room temperature while, the high value of the dipole moment for the C_I conformer could in part explain it stability, as was observed in other molecules [39-44]. In PE, the absence of the CF_2H group decrease the dipole moment value up to 2.04 D while its direction undergoes a significant change toward right in approximately 45°, as can be seen in Figure S3. In relation to TFPE, note that the CF_3 group increase the dipole moment up to 2.72 D while the direction slightly change toward left in approximately 20°, as can be seen in Figure S3. Thus, the results show that the addition of F atoms in the structures of DFPE and TFPE produce considerable variations in the directions of the dipole moments due to the charges that modifications in the distances between centre of positive and negative charges (0.68-0.52 D).

The calculated geometrical parameters for the three theoretical structures of DFPE were compared with those experimental reported for the 2-acetylepyrrol [45] and for 2-(difluoromethyl) isonicotinonitrile [1] by means of the root-mean-square deviation (RMSD) values which are summarized in Table 1.

The calculated bond lengths and angles for the three conformers of DFPE by using the B3LYP/6-31G* method show a good correlation with those experimental values with rmsds values, for the distances of 0.019 Å and, for the angles between 0.6 and 0.7°. Therefore, these results provide a reliable starting point for the frequency calculations and B3LYP/6-31G* force field of DFPE. Experimentally, 2-acetylepyrrol [45] forms centro symmetric dimers in the solid state, through N-H--O hydrogen bonds involving amine and carbonyl groups, for this reason, in the PE, DFPE and TFPE solids similar structures could be expected.

Charges and molecular electrostatic potentials studies

As was mentioned above, in DFPE there are two potentials hydrogen bond donors sites, characterized by the N-H and F_2C-H groups, for which, it is very important to know which of them is the strongly donor site because the only acceptor site is that determined by the C=O group. Hence, for the three conformers of DFPE, the molecular electrostatic potentials together with the NPA and MK' charges were analyzed. The calculated molecular electrostatic potentials and the two

B3LYP/6-31G* Methoda				
Parameter	C1	c2	C3	Exp.
Bond Length (Å)				
C1=C2	1.390	1.389	1.389	1.366
C2=C3	1.411	1.411	1.412	1.394
C3=C4	1.393	1.393	1.394	1.380
C4=N5	1.373	1.375	1.376	1.369
N5=C1	1.361	1.360	1.360	1.349
C1-C9	1.486	1.492	1.492	
C4 -C13	1.466	1.464	1.465	1.445
C13 -C14	1.516	1.516	1.516	1.500
N5 –H6	1.011	1.011	1.012	0.914
C13=O18	1.227	1.228	1.228	1.227
C9 –F11	1.373	1.364	1.374	1.371[c]
C9 – F12	1.372	1.374	1.365	1.372[c]
C9 –H10	1.094	1.096	1.097	1.000
C14 –H15	1.091	1.091	1.091	0.965
C14 –H16	1.096	1.096	1.096	0.999
C14 –H17	1.096	1.096	1.096	0.932
C2 –H7	1.081	1.080	1.081	0.981
C3 -H8	1.081	1.081	1.082	0.949
RMSD	0.019	0.019	0.019	
Bond angle (degrees)				
H10-C9-F11	107.9	107.4	106.9	110.5[c]
H10-C9-F12	108.8	106.9	107.4	110.5[c]
F11-C9-F12	106.6	109.0	109.0	105.8[c]
H10-C9-C1	112.5	114.3	114.3	110.5
F11-C9-C1	111.2	109.8	109.3	109.4[c]
F12-C9-C1	109.6	109.3	109.8	110.0[c]
C9-C1-C2	130.3	130.3	130.3	
C9-C1-N5	121.6	121.4	121.4	
C1-C2-H7	125.7	125.5	125.5	127.4
C1-C5-H6	127.3	127.3	127.3	123.0
H7-C2-C3	127.1	127.5	127.5	125.2
H6-N5-C4	122.6	122.6	122.6	127.5
H8-C3-C4	125.9	125.8	125.8	126.0
C3-C4-C13	134.0	134.2	134.2	131.4
N5-C4-C13	118.7	118.6	118.6	121.6
C4-C13-O18	119.8	119.8	119.8	
C4-C13-C14	118.1	118.1	118.1	118.2
O18-C13-C14	122.1	122.1	122.1	
C13-C14-H15	109.1	109.0	109.0	110.6
C13-C14-H16	110.7	110.7	110.8	112.5
C13-C14-H17	110.8	110.8	110.7	113.9
RMSD	0.6	0.7	0.7	
C2-C1-C9-H10	-24.948	-86.535	86.432	
C2-C1-C9-F11	96.212	34.246	-153.825	
C2-C1-C9-F12	-146.189	153.72855	-34.338	
N5-C1-C9-H10	158.823	88.725	-88.814	
N5-C1-C9-F11	-80.015	-150.494	30.928	
N5-C1-C9-F12	37.582	-31.011	150.415	
C3-C4-C13-O18	178.794	-179.148	179.121	
N5-C4-C13-O18	-0.279	0.006	0.011	
C4-C13-C14-H15	179.290	179.004	-178.858	
C4-C13-C14-H16	-60.267	-60.588	-58.234	
C4-C13-C14-H17	58.702	58.397	60.751	
O18-C13-C14-H15	-0.806	-1.064	1.223	
O18-C13-C14-H16	119.635	119.344	121.847	
O18-C13-C14-H17	-121.394	-121.671	-119.168	
H6-N5-C4-C13	1.492	-2.912	2.859	0.31
H8-C3-C4-C13	0.797	-0.754	0.798	1.88

[a]This work
[b]From Ref [45]
[c]From Ref [1]

Table 1: Comparison of calculated geometrical parameters with the corresponding experimental values for the conformers of 1-(5-(difluoromethyl)-1H-pyrrol-2-yl) ethanone.

types of charges are presented in Table S4 and S5, respectively. In this study, the results for DFPE were compared with those calculated for TFPE. As expected, the higher molecular electrostatic potential values are observed on the F11, F12, O18 and N5 atoms while the lower values on the H6 and H10 atoms. Note that the H6 atoms belonging to the NH groups are the strongest donor sites in relation to the F_2CH sites because the N atoms are most electronegative than the C ones. On the other hand, analyzing the atomic charges, the H6 atoms have the most positive NPA and MK charges, in reference to the H10 atoms of the three conformers of DFPE, while the charges on the O18 atoms confirm that these sites are clearly the acceptor sites in DFPE. Note that the MK charges on all the atoms have lower values than the other ones, as observed in other molecules [43,46-49]. Figure S4 show the most negative potential on the O18 atoms and the most positive on the H6 atoms, thus, the strong red colour is observed on the acceptor C=O sites indicating probable capability of hydrogen bond formation while the strong blue colour is observed on the two donor N-H and F_2C-H sites. Additionally, these calculations show practically the same values for the C_{II} and C_{III} conformers, as was also observed in their energies and dipole moment values. The comparison with TFPE values show that the molecular electrostatic potential and the charges values are slightly lower on practically all the atoms of TFPE, as can be seen in Tables S4 and S5, revealing that the presence of a CF_3 group in this compound increase the donor effect of the NH group belonging to the pyrrol ring. Later, in the structure of DFPE solid intermoleculars NH--- N or CO---H bonds are expected.

NBO study

The above analyses show that the C=O groups are related with nucleophilic sites in DFPE while the N-H and F_2C-H groups with two possible donor sites, being the N-H sites the strongest donor in that molecule. The calculations related with the bond orders, which are expressed as Wiberg indexes, can be seen in Table S6. The values also show that the H6 atoms have lower bond order values than the H10 atoms confirming, thus, that the NH bonds are weaker than the F_2C-H bonds. In the three conformers, the bond orders calculated for the O atoms have the same values due to their double bonds character. Note that the C_{II} and C_{III} conformers also, as in the above cases have the same bond order values. In TFPE, the presence of the CF_3 group not shows significant changes in the bond order values, in reference to DFPE.

Moreover, taking into account the presence of pyrrol rings in the three conformers of DFPE and, of lone pairs due to the N5, F11, F12 and O18 atoms, the stabilization energies associated with delocalization energetic by NBO analysis was carried out in order to estimate all possible interactions between "filled" (donor) Lewis-type NBOs and "empty" (acceptor) non-Lewis NBOs [15,16]. Thus, the calculated main delocalization energies can be seen in Table S7. The results show two different interactions related with the C=C bonds belonging to the pyrrol rings and with the lone pairs of the N5, F11, F12 and O18 atoms. These interactions are the $\Delta E\ \sigma \rightarrow \sigma^*$ and $\Delta ELP \rightarrow \sigma^*$ charge transfers, where the latter delocalizations have the higher values, contributing thus in great part to the ΔE Total. Note that the total energies of the C_I and C_{III} conformers are the same and slightly higher than C_I, justifying its probable presence at room temperature, as was thermodynamically observed in the section 3.1. In TFPE, the existence of the CF_3 group shows significant changes due to the presence of other F atom and, as consequence, increases the total stabilization energy in this compound, as compared with DFPE.

AIM analysis

The hydrogen bonding plays an important role in the design of bioactive molecules and, as in DFPE there are nucleophilic and electrophilic sites it is expected the presence of probable inter and/or intra-molecular interactions and, in additional form, the possibility of it for act as a pharmacologic drug. For these reasons, for the three conformers of DFPE was performed a topological analysis by means the AIM2000 program [18]. The electron charge density, (ρ) and the Laplacian of the electron density, $\nabla^2\rho(r)$ calculated for the three conformers of DFPE show the presence only of ring critical points (RCPs) whose properties can be seen in Table S8. Here, the topological properties for the C_I conformer have slightly higher values than C_{II} and C_{III} while the same values are observed in these last two conformers. This analysis clearly shows that the three conformers are expected in the gas phase and that in their structures intra-molecular interactions are not observed. Additionally, the presence of the CF_3 group slightly increases the electron charge density of TFPE, as compared with the three conformers of DFPE (Table S8). The latter result is expected due to the presence of three electronegative F atoms in TFPE. It is important to mentioned that the AIM analysis for the three conformers of DFPE by using the 6-311++G** neither show bond critical points in their structures and, therefore, intra-molecular interactions are not observed by using this level of theory.

NMR analysis

A comparison of the theoretical ^{1}H-NMR, ^{13}C-NMR, ^{19}F-NMR chemical shifts for the three conformers of DFPE, calculated employing the GIAO and CGST methods [27,28] at the B3LYP/6-311++G** level, with the corresponding experimental values by means of the root mean square deviations (RMSD) values can be seen in Table 2. In general, the calculated chemical shifts with both methods show higher values than the corresponding experimental ones, as also was observed in other molecules [4,50-54]. In both cases, the results show a good concordance for the H nuclei with rmsd values between 0.8 and 0.9ppm and a slightly lower agreement for the ^{13}C nuclei (4.9-4.1 ppm) while the calculated ^{19}F chemical shifts show the higher rmsd values using the GIAO method (18.2 and 20.8 ppm) and the lower values using the CGST method. These observed higher variations can be attributed in part to the calculations because they were performed in gas phase while the experimental values were obtained for DFPE in solution.

^{1}H-NMR							
B3LYP/6-311++G**							
Atoms	GIOA method			CGST method			δ (ppm)
	C1	C2	C3	C1	C2	C3	Exp[b]
H 6	9.21	8.92	8.92	9.13	8.78	8.78	6.88
H 7	6.40	6.43	6.43	6.50	6.61	6.61	
H 8	6.70	6.77	6.78	6.88	6.92	6.92	6.50
H 15	2.09	2.05	2.05	2.57	2.52	2.52	
H 16	2.57	2.55	2.56	3.05	3.02	3.02	2.47
H 17	2.57	2.56	2.55	3.05	3.02	3.02	
H 10	6.59	6.93	6.93	6.64	7.00	7.00	6.73
RMSD	0.9	0.8	0.8	0.9	0.8	0.8	
^{13}C-NMR							
C 1	135.5	136.2	136.2	134.2	134.6	134.6	130.7
C 2	115.6	114.4	114.4	114.4	113.7	113.7	109.6
C 3	118.1	119.1	119.1	117.3	118.4	118.4	110.4
C 4	138.9	138.4	138.4	136.9	136.7	136.7	133.2
C 9	115.8	117.1	117.0	115.3	115.5	115.5	117.2
C 13	192.5	192.2	192.2	192.0	191.6	191.6	189.0
C 14	26.1	25.9	25.9	26.4	26.2	26.2	25.8
RMSD	4.9	4.9	4.9	4.0	4.1	4.1	
^{19}F-NMR							
F 11	106.1	131.4	133.6	101.3	126.8	128.6	
F 12	136.8	133.5	131.3	132.2	128.5	126.8	111.7
RMSD	18.2	20.8	20.8	16.3	16.0	16.0	

[a]GIAO/B3LYP/6-311++G** and CGST/ B3LYP/6-311++G** Ref. to TMS
[b]From Ref [1] Ref. to CD_3OD
[c]GIAO/B3LYP/6-311++G** and CGST/ B3LYP/6-311++G** Ref. to CCl_3F

Table 2: Observed and calculated H, C and F chemical shifts (δ, in ppm) for the three conformers of 1-(5-(difluoromethyl)-1H-pyrrol-2-yl) ethanone.

On the other hand, the GIAO method uses basis functions which depend on the field while the CSGT method achieves gauge invariance by performing a continuous set of gauge transformations, for each point, obtaining an accurately description of the current density [53]. Additionally, the proximities between the values for the three conformers suggest their presence in solution. A further observation is that the peak belonging to the H atom of the N-H bond appears in furyl compounds at 11.37 ppm [50-53], in this case for the N5-H6 bonds are observed at 6.88 ppm, as in the 2-(2'- furyl)-1H-imidazole compound [52,53]

whose crystalline structure is polymeric with N-H---N bonds. Thus, the small shifts of these peaks towards lower fields suggest for DFPE probably the existence of some intermolecular interaction between nonbonding electrons.

Vibrational analysis

In this analysis, we considered the three stable structures of DFPE because they are thermodynamically predicted due to the proximities in their energy values. The three DFPE conformers and the TFPE structure have 48 normal vibration modes and all the modes are active in the IR and Raman spectra. The predicted IR and Raman spectra for the three conformers of DFPE by using B3LYP/6-31G* level can be seen in Figures 2 and 3, respectively compared with the corresponding to TFPE. The experimental bands observed in the infrared spectra in solid phase for DFPE and TFPE were taken from [1] and [24] and they are compared with the corresponding calculated wavenumbers in Table 3. The complete vibrational assignments of the experimental bands to the normal vibration modes were performed by comparison with related molecules [3,4,20-22,42,49-55] and taking into account the calculations performed here. The PED contributions for the three DFPE conformers can be seen in Tables S9- S11 while for TFPE are observed in Table S12. The comparison between the theoretical IR spectra show principally differences in the bands related to the vibration modes of the CF_2H and CF_3 groups, as observed in Figures 2 and 3 and, in Table 3. The SQM force fields for all the conformers of DFPE and for TFPE can be obtained at request. At continuation a brief discussion of the assignments of the most important groups is presented below.

DFPE and TFPE Assignments

C-H modes: In furyl imidazole compounds [50-53], the C-H stretchings are observed in the 3150-3012 cm^{-1} region, for this reason, the band observed at 3247 cm^{-1} is assigned to those vibration modes for the three conformers of DFPE while for TFPE these modes are associated with the band at 3254 cm^{-1}. For the C_I conformer these modes are calculated as totally pure while for the C_{II} and C_{III} conformers are observed combined between them. The in-plane deformation modes are observed between 1227 and 1018 cm^{-1} while the corresponding out-of-plane deformations of the C-H group are observed between 753 and 718 cm^{-1}. Hence, the IR bands at 1228 and 1094 cm^{-1} are assigned to those deformation modes for the three conformers, as observed in

Citation: Cataldo PG, Castillo MV, Brandán SA (2014) Quantum Mechanical Modeling of Fluoromethylated-pyrrol Derivatives a Study on their Reactivities, Structures and Vibrational Properties. J Phys Chem Biophys 4: 133. doi:10.4172/2161-0398.1000133

1-(5-(difluoromeτhyl)-1H-pyrrol-2-yl) eτhanone[a]										1-(5-(τrifluoromeτhyl)-1H-pyrrol-2-yl) eτhanone[a]			
Exp[b]	C_I			C_{II}				C_{III}					
IR	Calc.[d]	SQM[e]	Assignmenτ	Calc.[d]	SQM[e]	Assignmenτ	Calc.[d]	SQM[e]	Assignmenτ	Exp[c] IR	Calc.[d]	SQM[e]	Assignmenτ
	3634	3483	ν(N5-H6)	3636	3485	ν(N5-H6)	3636	3485	ν(N5-H6)		3630	3480	ν(N5-H6)
	3273	3138	ν_{ip}(C-H)	3279	3143	ν_{ip}(C-H)	3279	3143	ν_{ip}(C-H)		3283	3147	ν_{ip}(C-H)
3247	3258	3123	ν_{op}(C-H)	3264	3129	ν_{op}(C-H)	3264	3129	ν_{op}(C-H)	3254	3267	3132	ν_{op}(C-H)
	3171	3039	$\nu_{as}CH_3$	3170	3039	$\nu_{as}CH_3$	3170	3039	$\nu_{as}CH_3$		3171	3040	$\nu_{as}CH_3$
	3115	2986	$\nu_{as}CH_3$	3115	2986	$\nu_{as}CH_3$	3115	2986	$\nu_{as}CH_3$		3116	2986	$\nu_{as}CH_3$
	3108	2979	ν(C9-H10)	3071	2944	ν(C9-H10)	3071	2944	ν(C9-H10)				
	3056	2929	ν_sCH_3	3056	2929	ν_sCH_3	3056	2929	ν_sCH_3	2923	3056	2929	ν_sCH_3
1645	1753	1688	ν(C13-O18)	1750	1685	ν(C13-O18)	1750	1685	ν(C13-O18)	1671	1755	1689	ν(C13-O18)
	1614	1559	ν(C1-C2)	1612	1556	ν(C1-C2)	1612	1556	ν(C1-C2)	1561	1613	1557	ν(C1-C2)
	1539	1490	βR_1	1542	1492	ν(C3-C4)	1543	1492	ν(C1-C9)		1544	1493	ν(C3-C4)
	1504	1450	ν(C1-N5)	1504	1440	ν(C1-N5)	1504	1440	ν(C1-N5)		1503	1438	δ_aCH_3
	1498	1439	δ_aCH_3	1497	1438	δ_aCH_3	1497	1438	δ_aCH_3		1497	1435	ν(C1-N5)
	1495	1433	δ_aCH_3	1482	1432	δ_aCH_3	1482	1432	δ_aCH_3		1481	1430	δ_aCH_3
	1459	1412	ν(C3-C4)	1457	1413	ν(C4-N5)	1457	1413	ν(C3-C4)		1454	1407	ν(C4-N5)
1376	1413	1370	ρ'(CH)	1413	1371	ρ'(CH)	1413	1371	ρ'(CH)				
	1400	1353	δ_sCH_3	1407	1357	ρ(CH)	1407	1357	ρ(CH)	1333	1413	1352	δ_sCH_3
	1385	1345	ρ(CH)	1393	1349	δ_sCH_3	1393	1349	δ_sCH_3		1375	1324	ν(C2-C3)
	1356	1309	ν(C2-C3)	1350	1304	ν(C2-C3)	1350	1304	ν(C2-C3)	1292	1302	1259	ν(C4-C13)
1228	1267	1235	β(-H)	1266	1233	βC-H)	1266	1233	βC-H)		1271	1239	βC-H)
	1255	1216	β(C-H)	1257	1219	ν(C4-C13)	1257	1219	β(-H)				
										1164	1219	1173	$\nu_{as}CF_3$
										1115	1180	1135	$\nu_{as}CF_3$
										1096	1169	1127	ν_sCF_3
	1136	1100	ν(C4-N5)	1144	1106	ν_sCF_2	1144	1106	ν(C4-N5)				
1094	1101	1067	ν_sCF_2	1137	1098	$\nu_{as}CF_2$	1137	1098	$\nu_{as}CF_2$		1103	1068	β(N-H)
	1089	1048	$\nu_{as}CF_2$	1094	1059	β(N-H)	1094	1059	ν_sCF_2				
	1075	1042	βC-H)	1075	1042	βC-H)	1075	1042	βC-H)	1049	1078	1045	βC-H)
	1054	1031	ρCH_3	1053	1031	ρCH_3	1053	1031	ρCH_3	1033	1054	1031	ρCH_3
1012	1019	994	βR_2	1014	991	βR_1	1014	991	βR_1		1005	983	βR_1;ρ'CH_3
	1004	982	ρ'CH_3	1003	978	ρ'CH_3	1003	978	βR_2		971	950	βR_2
931	943	919	ν(C13-C14)	942	919	βR_2	943	919	ρ'CH_3		938	917	ν(C13-C14)
	872	863	γ(C3-H8)	880	870	γ(C3-H8)	880	870	γ(C3-H8)		882	873	γ(C2-H7)
805	807	795	γ(C2-H7)	837	826	wag(CF_2)	837	826	wag(CF2)				
780	797	786	wag(CF_2)	797	787	γ(C2-H7)	797	787	γ(C2-H7)	795	808	799	γ(C3-H8)
										738	736	709	δ_sCF_3
	715	697	τR_2	697	680	τR_2	697	680	τR_2		721	701	τR_2
	675	658	τR_1	658	644	τR_1	658	644	γ(N5-H6)		678	661	τR_1
	633	623	γ(N5-H6)	636	623	ν(C13-C14)	636	623	ν(C13-C14)		641	624	β(C=O)
	625	612	βC=O)	609	594	γ(N5-H6)	609	594	τR_1		623	615	γ(N5-H6)

											581	562	$\delta_a CF_3$
	577	568	δCF_2	559	548	δCF_2	559	548	δCF_2		560	544	γ(C13-O18)
	555	541	γ(C13-O18)	544	533	γ(C13-O18)	544	533	γ(C13-O18)		531	512	$\delta_a CF_3$
	514	505	ν(C4-C13)	525	517	δCCC	525	517	δCCC		512	502	δCCC
	433	424	$\rho(CF_2)$	479	470	βC=O)	479	470	$\rho(CF_2)$		440	429	βC=O)
	399	393	ν(C1-C9)	401	395	ν(C1-C9)	401	395	βC=O)		402	390	$\rho' CF_3$
											384	372	ρCF_3
	356	350	ρC_9-C_1	307	301	βC=O)	307	301	ν(C4-C13)		291	284	ν(C1-C9)
	217	215	δCCC	214	212	γ(C1-C9)	215	212	γ(C1-C9)		211	210	ρC13-C4
	189	186	γ(C13-C4)	210	209	ρC13-C4	210	209	ρC13-C4		188	185	γ(C13-C4)
	136	127	γ(C1-C9)	143	135	γ(C13-C4)	143	135	γ(C13-C4)		135	126	τw(CC)
	113	112	ρC_{13}-C_4	114	113	ρC_9-C_1	114	113	ρC9-C1		108	107	ρC9-C1
	84	79	$\tau w(CH_3)$	86	80	τw(CC)	86	80	τw(CC)		82	76	γ(C1-C9)
	60	54	τw(CC)	49	45	$\tau w(CH_3)$	49	45	$\tau w(CH_3)$		56	50	$\tau w(CH_3)$
	32	31	$\tau w(CF_2)$	34	29	$\tau w(CF_2)$	34	29	$\tau w(CF_2)$		22	20	$\tau w(CF_3)$

[a]This work
[b]From Ref. [1]
[c]From Ref [24]
[d]From B3LYP/6-31G* method
[e]From scaled quantum mechanics force field

Table 3: Experimental and calculated frequencies (cm^{-1}) and assignment of the three conformers of 1-(5-(difluoromethyl)-1H-pyrrol-2-yl) ethanone and for 1-(5-(trifluoromethyl)-1H-pyrrol-2-yl) ethanone.

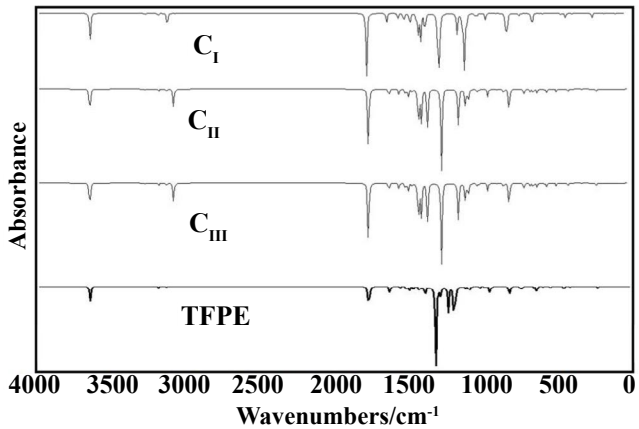

Figure 2: Comparison between the theoretical infrared spectra of the three stable conformers of 1-(5-(difluoromethyl)-1H-pyrrol-2-yl) ethanone (DFPE) at B3LYP/6-31G* level of theory with the corresponding to 1-(5-(trifluoromethyl)-1H-pyrrol-2-yl) ethanone (TFPE) at the same level of theory.

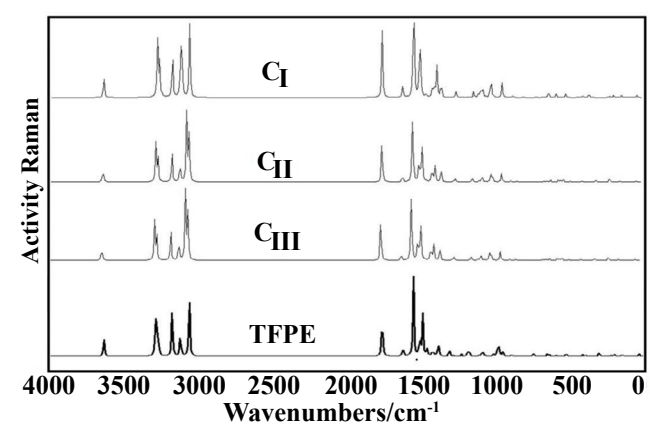

Figure 3: Comparison between the theoretical Raman spectra of the three stable conformers of 1-(5-(difluoromethyl)-1H-pyrrol-2-yl) ethanone (DFPE) at B3LYP/6-31G* level of theory with the corresponding to 1-(5-(trifluoromethyl)-1H-pyrrol-2-yl) ethanone (TFPE) at the same level of theory.

Table 3. For TFPE, only one in-plane deformation mode and one out-of-plane deformation mode were assigned to the bands at 1049 and 795 cm-1, respectively.

Note that the calculated C-H stretchings wavenumbers for C_{II} and C_{III} by using SQM calculations have higher values than C_I while the two C-H rocking modes corresponding to the CF_2H groups are predicted at the same wave numbers.

CH_3 modes: As observed in molecules containing this group [20,42,49,54,55], both anti-symmetric and symmetric stretchings modes are predicted for the three conformers of DFPE and TFPE as totally pure modes in the expected region. Thus, taking into account this observation, those modes were assigned in the same region. Note that only the symmetric stretching and the bending modes for TFPE were assigned to the bands at 2923 and 1333 cm^{-1}. Furthermore, the rocking and twisting modes of the methyl group for DFPE and TFPE were predicted by the calculations in the same regions and, for these reasons, they were assigned accordingly.

NH modes: Note that the presence of the CF_3 group in TFPE produce a shifting of the N-H stretching mode toward lower wavenumbers, thus, the SQM calculations predict this stretching mode at 3480 cm^{-1}

while in the three conformers of DFPE are predicted between 3485 and 3433 cm^{-1}. Moreover, the IR and Raman bands attributed to the N-H stretching mode in the C_I conformer is predicted with higher intensity than in the other ones, as can be seen in Figures 2 and 3. For DFPE and TFPE, the in-plane and out-of-plane deformation modes are predicted in the regions between 1219-1068 and 873-797 cm^{-1}, respectively.

CF_2 and CF_3 modes: The more important variations in the IR spectra of DFPE and TFPE are observed for the vibration modes of these groups [55]. Thus, both CF_2 stretchings modes for the three conformers of DFPE are predicted by SQM calculations between 1048 and 1098 cm^{-1} and, for this, they were assigned to the band at 1094 cm^{-1}. For TFPE, the three CF_3 stretchings modes are clearly assigned to the bands at 1164, 1115 and 1096 cm^{-1}. Only, the CF_3 symmetric deformation mode was assigned to the band at 738 cm^{-1} while, the two rocking and twisting modes were predicted respectively at 402, 384 and 22 cm^{-1}. For the three conformers of DFPE, only were assigned the wagging modes at 805 and 780 cm^{-1} while the rocking and twisting mode are predicted between 479-424 and 34-29 cm^{-1}, as observed in Table 3.

Skeletal modes: The C-C and C-N stretching modes belonging to the pyrrol ring undergoes slightly changes in the intensities and positions of the bands due to the presence of the CF_2 and CF_3 groups while, the C-C and C=O stretching modes belonging to the side chain of DFPE and TFPE are predicted by SQM calculations in the same regions. Hence, the C13-O18 stretching modes in DFPE are assigned to the band at 1645 cm^{-1} while in TFPE that mode is assigned to the band at 1671 cm^{-1}. Figures 2 and 3 shows clearly that the IR and Raman bands attributed to the C=O stretching modes of the three conformers of DFPE are predicted with higher intensities than the corresponding to TFPE. The C1-C2 stretching modes in DFPE are predicted between 1559 and 1556 cm^{-1} while in TFPE that mode is assigned to the band at 1561 cm^{-1}. The positions of the bands assigned to the two ring deformation and torsion modes corresponding to the pyrrol ring are also slightly modified as consequence of the CF_2 and CF_3 groups, as can be observed in Table 3. Thus, the bands observed in the spectrum of DFPE at 1012 and 931 cm^{-1} can be assigned to ring deformation modes corresponding to the conformers of DFPE, in accordance with the calculations.

Force Field

The force constants for the three conformers of DFPE were calculated at the B3LYP/6-31G* level of theory by using the SQM methodology [26] with the Molvib program [34]. The values for DFPE are observed in Table 4 compared with those calculated for TFPE.

The results show, on one hand, that the force constants related with the C-N, C-C and C-H stretchings belonging to the pyrrol rings for the three conformers of DFPE are different from those calculated for TFPE as consequence of the CF_2 and CF_3 groups. On the other hand, these groups have not influence on the side chain because the CH_3 stretchings force constants values are not modified while the C=O stretchings force constants values are slightly different in DFPE and TFPE, as observed in Table 4. These observations are probably related to the different intensities and positions of the bands associated with the C=O stretchings modes in DFPE and TFPE, as explained in the vibrational analysis (Table 3). The presence of three F atoms in TFPE justifies the high C-F stretching force constant value in TFPE, in relation to DFPE.

Force constant	1-(5-(difluoromethyl)-1H-pyrrol-2-yl) ethanone (DFPE)[a]			1-(5-(trifluoromethyl)-1H-pyrrol-2-yl) ethanone (TFPE)[a]
	C_I	C_{II}	C_{III}	
$f(\nu C{=}N)_{Ring}$	6.522	6.525	6.525	6.551
$f(\nu C\text{-}C)_{Ring}$	6.438	6.437	6.437	6.458
$f(\nu C\text{-}C)$	4.443	4.446	4.447	4.467
$f(\nu C\text{-}F)$	5.268	5.374	5.374	5.608
$f(\nu CH_3)$	4.919	4.918	4.918	4.920
$f(\nu C{=}O)$	11.445	11.399	11.398	11.467
$f(\nu N\text{-}H)$	6.724	6.731	6.731	6.710
$f(\nu C_9\text{-}H_{10})$	4.880	4.775	4.775	
$f(\nu C\text{-}H)$ Ring	5.361	5.379	5.379	5.391
$f(\delta CF_2, CF_3)$	1.887	1.759	1.759	1.417

Units are mdyn $Å^{-1}$ for stretching and stretching/stretching interaction and mdyn Å rad^{-2} for angle deformations

[a]This work at the B3LYP/6-31G* level of theory

Table 4: Comparison of scaled internal force constants for DFPE with the corresponding to TFPE.

Descriptors Predicted

In order to predict the behaviours of the three conformers of DFPE in gas phase the HOMO and LUMO orbitals and the energy band gaps were calculated together with some descriptors, such as chemical potential (μ), electronegativity (χ), global hardness (η), global softness (S) and global electrophilicity index (ω) [19,46,56]. The presences in DFPE of electrophiles and nucleophiles sites are very important to understand the behaviours and reactivities of these species in the drug design. The comparison of these descriptors with molecules without the CF_2H group (PE) and with the CF_3 group (TFPE) is essential to understand the influence of both groups on the structures and properties of these compounds. A comparison of the obtained values for DFPE by using B3LYP/6-31G* level of theory with those computed in this work at the same calculation level for 1-(1H-pyrrol-2-yl) ethanone and 1-5-(trifluoromethyl-1H-pyrrol-2- yl-) ethanone can be seen in Table S13. Comparing the energy band gaps for the conformers of DFPE (-5.072 and -5.080 eV) with the calculated value for 1-(1H-pyrrol-2-yl) ethanone of -5.064 eV, we observed that the absence of the CF_2H group in this compound genera the slightly reduction of the HOMO-LUMO gap indicating that PE is more reactive than DFPE. On the contrary, the comparison of DFPE with TFPE indicates that the gap energy increasing due to the CF3 group, for this, DFPE is more reactive than TFPE, as observed by NBO analysis. On the other hand, comparing the calculated chemical hardness η (2.540-2.536 eV), chemical potential μ (-3.939- -3.875eV) and global electrophilicity index ω (3.054-2.960 eV) values for DFPE with those obtained for PE of 2.532, -3.544 and 2.481 eV, we observed that DFPE is more stable (larger η) and has better capability to accept electrons (bigger electrophilicity index) than PE. On the contrary, comparing those values for DFPE with the obtained for TFPE of 2.561, -4.109 and 3.297 eV clearly the compound with the CF_3 group is more stable and has better capability to accept electrons than DFPE. These latter results are supported by the strong electronegativities of the F atoms in TFPE, as observed by the molecular electrostatic potentials.

Conclusions

In the present work, the theoretical molecular structures of the three conformers of 1-(5- (difluoromethyl)-1H-pyrrol-2-yl) ethanone and the more stable structures of 1-(5- (trifluoromethyl)-1H-pyrrol-2-yl) ethanone were determined in gas phase by using the B3LYP/6-31G* method. The B3LYP/6-31G* calculations in gas phase suggest that the three conformations can exist in the solid phase due to the

low energies difference among them. The charges and molecular electrostatic potentials analyses predict intermolecular NH---N or CO---H bonds in the structure of 1-(5-(difluoromethyl)-1H- pyrrol-2-yl) ethanone solid. The NBO and AIM studies demonstrates that the total stabilization energy and the topological properties increases in 1-(5-(trifluoromethyl)-1H-pyrrol-2-yl) ethanone due to the presence of the CF_3 group. The SQM force fields for 1-(5-(difluoromethyl)-1H-pyrrol-2-yl) ethanone and 1-(5-(trifluoromethyl)-1H- pyrrol-2-yl) ethanone were calculated and the complete assignments for the 48 normal modes of vibration corresponding to both compounds are reported together with their corresponding force constants. The comparison among the different descriptors of the 1- (1H-pyrrol-2-yl) ethanone, 1-(5-(difluoromethyl)-1H-pyrrol-2-yl) ethanone and 1-(5-(trifluoromethyl)-1H-pyrrol-2-yl) ethanone compounds show that (i) the gap energies following the trend: ΔEGapPE < ΔEGapDFPE < ΔEGapTFPE, (ii) the electrophilicity index following the trend: PE < DFPE < TFPE and, (iii) the compound with the CF3 group has better capability to accept electrons due to their bigger electrophilicity index and, additionally, it has a low reactivity.

Acknowledgement

This work was founded with grants from CIUNT (Consejo de Investigaciones, Universidad Nacional de Tucumán). The authors thank Prof. Tom Sundius for his permission to use MOLVIB.

Supporting Information Available

Tables S1-S13 and Figures S1-S4 are included in the Supporting Information.

References

1. Fujiwara Y, Dixon JA, Rodriguez RA, Baxter RD, Dixon DD, et al. (2012) A new reagent for direct difluoromethylation. J Am Chem Soc 134: 1494-1497.
2. Erickson JA, McLoughlin JI (1995) Hydrogen Bond Donor Properties of the Difluoromethyl Group. J Org Chem 60: 1626-1631.
3. Romano E, Davies L, Brandán SA (2013) Structural and vibrational studies and molecular force field of zinc difluoromethanesulfinate. J Mol Struct 1044: 144-151.
4. Romano E, Ladetto MF, Brandán SA (2013) Structural and vibrational studies of the potential anticancer agent, 5-difluoromethyl-1,3,4-thiadiazole-2-amino by DFT calculations. Comput Theoret Chem 1011: 57-64.
5. http://www.sogang.ac.kr/english/academic/03_under_0117.html
6. Billes F, Podea PV, Mohammed-Ziegler I, Tosa M, Mikosch H, et al. (2009) Formyl- and acetylindols: vibrational spectroscopy of an expectably pharmacologically active compound family. Spectrochim Acta A Mol Biomol Spectrosc 74: 1031-1045.
7. Diaw AKD, Yassar A, Gningue-Sall D (2008) New synthesis routes, characterization, electrochemical and spectral properties of p-substituted N-phenylpyrroles. Substituent effects. JJ Aaron ARKIVOC 2008: 122-144.
8. Soloducho J, Doskocz J, Cabaj J, Roszak S (2003) Practical synthesis of bis-substituted tetrazines with two pendant 2-pyrrolyl or 2-thienyl groups, precursors of new conjugated polymers. Tetrahedron 59: 4761-4766.
9. Pozo-Gonzalo C, Pomposo JA, Rodriguez J, Yu.Schmidt E, Vasil'tsov AM, et al. (2007) Synthesis and electrochemical study of narrow band gap conducting polymers based on 2,2′-dipyrroles linked with conjugated aza-spacers. Synth Met 157: 60-65.
10. Muller K, Faeh C, Diederich F (2007) Fluorine in pharmaceuticals: looking beyond intuition. Science 317: 1881-1886.
11. Furuya T, Kamlet AS, Ritter T (2011) Catalysis for fluorination and trifluoromethylation. Nature 473: 470-477.
12. Park BK1, Kitteringham NR, O'Neill PM (2001) Metabolism of fluorine-containing drugs. Annu Rev Pharmacol Toxicol 41: 443-470.
13. Becke AD (1993) Density functional thermochemistry. III. The role of exact exchange. J Chem Phys 98: 5648-5652.
14. Lee C, Yang W, Parr RG (1988) Development of the Colle-Salvetti correlation-energy formula into a functional of the electron density. Phys Rev B Condens Matter 37: 785-789.
15. Reed AE, Curtis LA, Weinhold F (1988) Chem Rev 88: 899-926.
16. Glendening ED, Badenhoop JK, Reed AD, Carpenter JE, Weinhold F (1996) NBO 3.1; Theoretical Chemistry Institute, University of Wisconsin; Madison, WI.
17. Bader RFW (1990) Atoms in Molecules, A Quantum Theory, Oxford University Press, Oxford, ISBN: 0198558651.
18. Biegler-Köning F, Schönbohm J, Bayles D (2001) Software news and updates. J Comput Chem 22: 545-559.
19. Parr RG, Pearson RG (1983) Absolute hardness: companion parameter to absolute electronegativity. J Am Chem Soc 105: 7512-7516.
20. Romano E, Raschi AB, Benavente A, BrandÃ¡n SA (2011) Structural analysis, vibrational spectra and coordinated normal of 2R-(-)-6-hydroxytremetone. Spectrochim Acta A Mol Biomol Spectrosc 84: 111-116.
21. Contreras CD, Ledesma AE, Lanús HE, Zinczuck J, Brandán SA (2011) Hydration of l-tyrosine in aqueous medium. An experimental and theoretical study by mixed quantum mechanical/molecular mechanics methods. Vibrat Spectr 57: 108-115.
22. Contreras CD, Montejo M, López González JJ, Zinczuk J, Brandán SA (2011) Structural and vibrational analyses of 2-(2-benzofuranyl)-2-imidazoline. J Raman Spectrosc 42: 108-116.
23. Brizuela AB1, Bichara LC, Romano E, Yurquina A, Locatelli S, et al. (2012) A complete characterization of the vibrational spectra of sucrose. Carbohydr Res 361: 212-218.
24. Ji Y, Brueckl T, Baxter RD, Fujiwara Y, Seiple IB, et al. (2011) Innate C-H trifluoromethylation of heterocycles. Proc Natl Acad Sci U S A 108: 14411-14415.
25. Fujiwara Y, Dixon JA, O'Hara F, Funder ED, Dixon DD, et al. (2012) Practical and innate carbon–hydrogen functionalization of heterocycles. Nature 492: 95-100.
26. Rauhut G, Pulay P (1995) Transferable Scaling Factors for Density Functional Derived Vibrational Force Fields. J Phys Chem 99: 3093-3100. b) Rauhut G, Pulay P (1995) Effect of Cetyltrimethylammonium Micelles with Bromide, Chloride, and Hydroxide Counterions on the Rates of Decomposition of Para-Substituted Aryl-2,2,2-trichloroethanols in Aqueous NaOH. [Erratum to document cited in CA123:9027]. J Phys Chem 99: 14572.
27. Ditchfield R (1974) Self-consistent perturbation theory of diamagnetism. Mol Phys 27: 789-807.
28. Keith TA, Bader RFW (1992) Calculation of magnetic response properties using atoms in molecules. Chem Phys Lett 194: 1-8.
29. Cheeseman J, Trucks G, Keith T, Frisch M (1996) A comparison of models for calculating nuclear magnetic resonance shielding tensors. J Chem Phys 104: 5497-5509.
30. Keith TA, Bader RFW (1993) Calculation of magnetic response properties using a continuous set of gauge transformations Chem Phys Lett 210: 223–231.
31. Nielsen AB, Holder AJ (2009) Gauss View 5.0, User's Reference, Gaussian Inc., Pittsburgh, PA.
32. Frisch MJ, Trucks GW, Schlegel HB, Scuseria GE, Robb MA (2009) J Gaussian Inc Pittsburgh, PA.
33. Besler BH, Merz Jr KM, Kollman PA (1990) Atomic charges derived from semiempirical methods. J Comp Chem 11: 431-439.
34. Sundius T (2002) Scaling of ab initio force fields by MOLVIB. Vib Spectrosc 29: 89-95.
35. Contreras CD, Ledesma AE, Zinczuk J, BrandÃ¡n SA (2011) Vibrational study of tolazoline hydrochloride by using FTIR-Raman and DFT calculations. Spectrochim Acta A Mol Biomol Spectrosc 79: 1710-1714.
36. Romano E, Soria NAJ, Rudyk R, Brandán SA (2012) Theoretical study of the infrared spectrum of 5-phenyl-1,3,4-oxadiazole-2-thiol by using DFT calculations. J Molec Simulation: 38: 561-566.
37. Leyton P, Brunet J, Silva V, Paipa C, Castillo MV, et al. (2012) An experimental and theoretical study of L-Tryptophan in an aqueous solution, combining two-layered ONIOM and SCRF calculations. Spectrochim Acta A Mol Biomol Spectrosc 88: 162-170.

38. Brizuela A1, Romano E, Yurquina A, Locatelli S, Brandan SA (2012) Experimental and theoretical vibrational investigation on the saccharinate ion in aqueous solution. Spectrochim Acta A Mol Biomol Spectrosc 95: 399-406.

39. Argañaraz GR, Romano E, Zinczuk J, Brandán SA (2011) J Chem & Chem Eng 5: 747-758.

40. Brandán SA, Benzal G, García-Ramos JV, Otero JC, Ben Altabef A (2008)Theoretical and experimental study of the vibrational spectra of 1,5-dimethylcytosine Vib Spec 46: 89-99.

41. Leyton P, Paipa C, Berrios A, Zárate A, Fuentes S, et al. J Mol Struct (2013) Structural study and characterization of the dipeptide 2-[[5-amino-5-oxo-2-(phenylmethoxycarbonylamino) pentanoyl] amino] acetic acid by vibrational spectroscopy and DFT calculations. J Mol Struct 1031: 110-118.

42. Roldán ML, Ledesma AE, Raschi AB, Castillo MV, Romano E, et al. (2013) Syntheses, spectral characterization, single crystal X-ray diffraction and DFT computational studies of novel thiazole derivatives. J Mol Struct 1041: 73-80.

43. Brandán SA, Eroglu E, Ledesma AE, Oltulu O, Yalçinkaya OB (2011) A new vibrational study of Acetazolamide compound based on normal coordinate analysis and DFT calculations. J Mol Struct 993: 225-231.

44. Romano E, Castillo MV, Pergomet JL, Zinczuk J, Brandán SA (2012) Synthesis and structural and vibrational analysis of (5,7-dichloro-quinolin-8-yloxy) acetic acid. J Mol Struct 1018: 149-155.

45. Camarillo EA, Flores H, Amador P, Bernès S (2007) Acta Cryst E63: o2593-o2594.

46. Márquez MB, Brandán SA (2013) A structural and vibrational investigation on the antiviral deoxyribonucleoside thymidine agent in gas and aqueous solution phases Int J Quan Chem 114: 209-221.

47. Romano E, Brizuela AB, Guzzetti K, Brandán SA (2013) An experimental and theoretical study on the hydration in aqueous medium of the antihypertensive agent tolazoline hydrochloride. J Mol Struct 1037: 393-401.

48. Guzzetti K, Brizuela AB, Romano E, Brandán SA (2013) Structural and vibrational study on zwitterions of l-threonine in aqueous phase using the FT-Raman and SCRF calculations. J Mol Struct 1045: 171–179.

49. Lizarraga E, Romano E, Raschi AB, Leyton P, Paipa C, et al. (2013) A structural and vibrational study of dehydrofukinone combining FTIR, FTRaman, UV–visible and NMR spectroscopies with DFT calculations. J Mol Struct 1048: 331–338.

50. Ledesma AE, Zinczuk J, López González JJ, Altabef AB, Brandán SA (2010) J Raman Spectrosc 41: 587–597.

51. Zinczuk J, Ledesma AE, Brandan SA, Piro OE, Lopez-Gonzalez JJ, et al. (2009) Structural and vibrational study of 2-(2′- furyl)-4,5-1H-dihydroimidazole J of Phys Org Chem. 22, 1166–1177.

52. Ledesma AE, Brandán SA, Zinczuk J, Piro OE, López González JJ, et al. , (2008) and vibrational study of 2-(2′-furyl)-1H-imidazole. Structural J of Phys Org Chem 21: 1086-1097.

53. Ledesma AE, Zinczuk J, López González JJ, Brandán SA (2012) Structural and Vibrational Properties and NMR characterization of (2'-furyl)-imidazole Compounds. Magnetic Resonance Spectroscopy Intech

54. Ledesma AE, Zinczuk J, López González JJ, Brandán SA, Ben Altabef A (2009) J Mol Struct: 924–926, 322–331.

55. Brandán SA, Ben Altabef A, Varetti EL (1999) An. Asoc Qca Arg 87: 89-96,

56. Chattaraj PK, Giri G (2009) Electrophilicity index within a conceptual DFT framework. Phys Chem 105: 13-39.